

This is the submitted version of the following article:

Ramirez-Priego P., Estévez M.-C., Díaz-Luisravelo H.J., Manclús J.J., Montoya Á., Lechuga L.M.. Real-time monitoring of fenitrothion in water samples using a silicon nanophotonic biosensor. *Analytica Chimica Acta*, (2021). 1152. 338276: - . 10.1016/j.aca.2021.338276,

which has been published in final form at
<https://dx.doi.org/10.1016/j.aca.2021.338276> ©
<https://dx.doi.org/10.1016/j.aca.2021.338276>. This manuscript version is made available under the CC-BY-NC-ND 4.0 license
<http://creativecommons.org/licenses/by-nc-nd/4.0/>

Real-time monitoring of fenitrothion in water samples using a silicon nanophotonic biosensor

Patricia Ramirez-Priego¹, M.-Carmen Estévez^{1,}, Heriberto J. Díaz-Luisravelo¹, Juan J.*

Manclús², Ángel Montoya² and Laura M. Lechuga¹

¹ Nanobiosensors and Bioanalytical Applications Group, Catalan Institute of Nanoscience and Nanotechnology (ICN2), CSIC, BIST and CIBER-BBN, Campus UAB, Bellaterra, 08193
Barcelona, Spain

² Centro de Investigación e Innovación en Bioingeniería (Ci2B), Universitat Politècnica de València, Camino de Vera s/n, 46022, Valencia, Spain

* Corresponding author. E-mail address: mcarmen.estevez@icn2.cat

KEYWORDS: silicon photonics, optical sensor, environmental monitoring, pesticide, organophosphate, fenitrothion, label-free.

ABSTRACT: Due to the large quantities of pesticides extensively used and their impact on the environment and human health, a prompt and reliable sensing technique could constitute an excellent tool for in-situ monitoring. With this aim, we have applied a highly sensitive photonic biosensor based on a bimodal waveguide interferometer (BiMW) for the rapid, label-free, and

specific quantification of fenitrothion (FN) directly in tap water samples. After an optimization protocol, the biosensor achieved a limit of detection (LOD) of 0.29 ng mL^{-1} (1.05 nM) and an IC_{50} of 1.71 ng mL^{-1} (6.09 nM) using a competitive immunoassay and employing diluted tap water. Moreover, the biosensor was successfully employed to determine FN concentration in blind tap water samples obtaining excellent recovery percentages with a time-to-result of only 20 minutes without any sample pre-treatment. The features of the biosensor suggest its potential application for real time, fast and sensitive screening of FN in water samples as an analytical tool for the monitoring of the water quality.

1. INTRODUCTION

Fenitrothion [O,O-Dimethyl O-(3-methyl-4-nitrophenyl) phosphorothioate] (FN) (Figure 1), is a powerful organophosphate (OP) insecticide used in large quantities because of its efficacy, cost-effectiveness, and availability [1]. This type of pesticide is extensively employed in agriculture and everyday household applications at worldwide level. Some of FN's applications include the control of a wide range of insects in cereals, rice, fruits, vegetables, store grains, and other crops, as well as in public health programs to control flies, mosquitoes, and cockroaches [2,3]. The uncontrolled use of organophosphate insecticides represents a relevant risk to the environment as they are potentially toxic to non-target organisms, including humans. Their main mechanism of action is based on the inhibition of the enzyme acetylcholinesterase involved in nerve impulse transmission [1,4]. Additionally, several studies have demonstrated that they are also carcinogenic [5], cytotoxic [6], mutagenic, genotoxic [7,8], and immunotoxic [9]. Toxicity of FN has been tested in mice, rats, Guinea pigs, and rabbits showing an oral lethal dose (LD_{50}) ranging between 250 and 870 mg Kg^{-1} [10,11]. In humans, the Food and Agriculture Organization of the United Nations (FAO), together with the World Health Organization (WHO) established an acceptable daily intake (ADI) of 0.005 mg Kg^{-1} [12]. Some of the chronic symptoms include general fatigue, headache, loss of memory, anorexia, nausea, and muscular weakness, among others [11]. For this reason, FN in particular, was recently banned in Europe and the United States; however, it is still used in Central and South America, Asia, and Africa [10,13,14]. Because of the toxicity of OP pesticides, including FN, the continuous monitoring in a wide range of samples such as soil, sediments, air, water, and food is crucial [15,16]. Indeed, one of the most common causes of human exposure is through drinking-water supplies due to pesticide leaching from contaminated soils to the groundwater [17]. WHO has published international standards for drinking water by publishing

Guideline Values (GV) for different pesticides. Although a GV for FN has not been given (judging by the occurrence of the pesticide at concentration well below those of health concern), a health-based value (HBV) of $8 \mu\text{g L}^{-1}$ [18,19]. can be calculated based on toxicity studies.

Conventional methods for the detection of FN and other OP pesticides include liquid and gas chromatography [20–22], mass spectroscopy [23,24], capillary electrophoresis [25], and Enzyme-Linked ImmunoSorbent Assay (ELISA) [26,27]. These methods are highly sensitive for the determination of OP pesticides. However, these techniques require laborious and time-consuming sample preparation and the use of bulky laboratory equipment and trained staff, making them unsuitable for in-field testing. To facilitate continuous routine analysis in real-time scenarios, the implementation of analytical tools that overcome these limitations and provide equal or even better levels of sensitivity are still in demand. Biosensors are one of the preferred options, as these devices can offer straightforward, rapid, portable, and low-sample and reagents consumption designs. Several electrochemical biosensors have been described for the detection of different OPs, including, chlorpyrifos, dichlorvos, parathion, and parathion-methyl, achieving a limit of detection (LOD) between 0.004 and 10 ng mL^{-1} [28–30]. Several examples have also been reported for the specific detection of FN. For instance, Ensafi *et al.* and Qi *et al.* employed an electrochemical sensor functionalized with graphene and metal oxide nanostructured material, achieving a LOD of 0.45 and 2.20 ng mL^{-1} , respectively, for FN in water samples [31,32]. Moreover, Kant also functionalized a Surface Plasmon Resonance (SPR) biosensor with similar nanostructures, reaching a LOD of 11.40 ng mL^{-1} in the case of FN in environmental samples [33].

We here propose the use of a highly sensitive photonic biosensor based on bimodal waveguide interferometers (BiMW) [34]. This design has already demonstrated numerous advantages over conventional methods, such as unprecedented sensitivity, rapid, label-free, and real-time

monitoring. Moreover, BiMW sensor chips are fabricated with standard microelectronics technology, enabling a reduction in fabrication costs and, therefore, in the final analysis cost. All the above advantages of the BiMW biosensor make this device an ideal candidate for on-site monitoring of OP pesticides. This BiMW device has already been employed for several clinical [35–38] and environmental [39,40] applications with real samples, for example for the specific detection of the biocide Irgarol 1051 in seawater, combining high specific custom-designed antibodies against the selected contaminant and the extreme sensitivity of the BiMW sensor [39]. The working principle of a BiMW biosensor relies on the interaction within the evanescent wave, an electromagnetic field associated to a monochromatic light propagating through the waveguide, which allows the excitation of two light modes [34]. These modes produce an interference pattern that is dependent on the local refractive index at the surface of the waveguide. Any event at the sensor surface, such as the binding of an analyte to its specific receptor, results in a change in the effective refractive index, which produces a phase shift between the two modes, and hence, an interference pattern that can be monitored in real-time.

In this work, we have optimized and validated the BiMW biosensor device to identify and quantify FN in tap water samples. The detection strategy consists of a competitive immunoassay by employing a highly specific monoclonal antibody produced against FN. The optimization of the immunosensor has been focused on two aspects: firstly, on improving the analytical parameters compared with routine detection methods and state-of-the-art biosensors, and secondly, on avoiding any previous sample pre-treatment or extraction for directly analyzing real water samples.

2. MATERIALS AND METHODS

2.1. Chemical and biological reagents

Organic solvents (acetone, ethanol, methanol, and ethanol absolute), hydrochloric acid (HCl, 37%), and nitric acid (HNO₃, 65%) were purchased from Panreac (Barcelona, Spain). Triethoxysilane polyethylene glycol carboxylic acid (silane-PEG-COOH, 600 Da) was supplied by Nanocs (New York, US). Reagents for carboxylic acid activation (N-(3-dimethylaminopropyl)-N'-ethylcarbodiimide hydrochloride (EDC) and N-hydroxysulfosuccinimide (sulfo-NHS)), 1,4-dioxane, fenitrothion (FN) analytical standard, bovine serum albumin (BSA), ovalbumin (OVA), and all reagents used for buffer preparation, hapten synthesis, and conjugation were provided by Sigma-Aldrich (Steinheim, Germany). The buffers employed were the following: phosphate buffer saline (PBS; 10 mM Na₂HPO₄, 1.8 mM KH₂PO₄, 2.7 mM KCl and 137 mM NaCl, pH 7.4), PBST (PBS with different concentrations of Tween 20, pH 7.4), MES buffer (0.1 M 2-(N-morpholino)ethanesulfonic acid (MES), pH 5.5), acetate buffer (10 mM pH 5.0), ethanolamine hydrochloride (1 M, pH 8.5). Milli-Q water was employed for all the buffers preparation.

2.2. Immunoreagents preparation.

Hapten FN4C (Figure 1) was prepared by the introduction of a ω -amino acid as an amide linkage of a suitable thiophosphate reagent, as previously described [41]. Briefly, ethyl dichlorothiophosphate was reacted with sodium 3-methyl-4-nitrophenolate followed by sodium 4-aminobutyrate. Finally, the thiophosphoramidate hapten was purified by column chromatography and its structure confirmed by nuclear magnetic resonance spectroscopy: ¹H NMR (CDCl₃) δ 8.03 (d, 1H, ArH5), 7.22 (m, 2H, ArH2,6), 4.19 (q+q, 2H, CH₂O), 3.39 (m, 1H, NH), 3.17 (m, 2H, CH₂N), 2.61 (s, 3H, ArCH₃), 2.46 (t, 2H, OOCCH₂), 1.88 (m, 2H, CH₂), 1.37 (t, 3H, CH₃). Hapten-protein conjugation (to BSA and OVA) was carried out by the N-hydroxysuccinimide-active ester method as described [41], and the conjugation was characterized by UV spectroscopy.

The hapten to protein molar ratio was estimated from hapten and protein spectral data. Apparent molar ratios of BSA- and OVA-FN4C conjugates were 18 and 4, respectively.

Monoclonal antibody (mAb) LIB-FN4C22 was obtained from mice immunized with the BSA-FN4C conjugate and applying the monoclonal antibody technology, essentially as described [41].

2.3. Bimodal waveguide sensor

The BiMW sensor chip (3 cm x 1 cm; Figure 2A) was fabricated in silicon nitride (Si_3N_4) at wafer-scale in a cleanroom facility, as previously described [34]. Each chip integrates an array of 20 independent bimodal waveguides. The working principle of the BiMW sensor relies on the behavior of light propagating through a waveguide, which allows only the propagation of the fundamental and first propagating modes of transverse electric polarized light (Figure 2A). In brief, light from a polarized diode laser ($\lambda = 660 \text{ nm}$; Hitachi; Tokyo, Japan) is first confined through the waveguide core in a single (fundamental) mode. After a certain distance, this fundamental mode is coupled into a bimodal section through a step junction that allows the appearance of the first propagating mode. These two modes travel across the sensing area and exit the waveguide. The evanescent field of the waveguide decays within the external medium and is altered by any change occurring on the close surface. This principle is exploited for sensing purposes. A sensing window is opened along the bimodal section of the waveguide, where the bioreceptors can be immobilized, and the detection occurs. Therefore, any refractive index change in this area, such as the one induced by the binding (or detachment) of any molecule, affects the propagating modes and results in an interferometric phase shift ($\Delta\phi$) between the two modes, modifying the intensity distribution at the sensor chip output. The intensity is recorded by a two-sectional photodetector (Hamamatsu Photonics, Hamamatsu, Japan) and processed through an acquisition card. An all-optical phase modulation method previously developed based on Fourier Series deconvolution is

applied [42], transforming the interference signal into a linear one able to continuously quantify the phase shifts between both modes. A fluidic system to ensure the liquid circulation to the sensing area is incorporated. It includes: a five-channel polydimethylsiloxane (PDMS) microfluidic cell (channel dimensions = 1.25 mm wide x 500 μm height) which is sealing the sensor chip, a syringe pump (New Era; New York, US) to guarantee a continuous flow rate of a running buffer, and a 6-port injection valve (VICI; Texas, US), that allows the sequential loading of the sample loop (100 μL) and injection of the different solutions.

2.4. Surface functionalization.

Before surface functionalization, the sensor chips were consecutively sonicated for 5 min in acetone, ethanol, milli-Q water, and 10 min in methanol/HCl 1:1 (v/v), to remove organic contamination. The sensor chips were then rinsed with water and dried with a stream of nitrogen. A layer of active hydroxyl groups was generated onto the sensor surface using oxygen plasma (Electronic Diener; Ebhausen, Germany) for 5 min at 45 sccm gas flow, followed by immersion in a 15% HNO_3 solution at 75 $^\circ\text{C}$ for 25 min. After rinsing generously with water and drying under N_2 flow, the sensor chip was immediately functionalized with silane-PEG-COOH, following the protocol previously detailed [35]. Briefly, the sensor chip was incubated with a solution of the silane (25 mg mL^{-1} in ethanol absolute/water 95:5 (v/v)) for 2 h at 4 $^\circ\text{C}$. After the incubation, the sensor chip was sequentially rinsed with ethanol and water and dried with a nitrogen stream. Finally, the sensor chip was subject to a curing process at high temperature, by placing it within a glass recipient and in a conventional autoclave for 90 min at 121 $^\circ\text{C}$ and a pressure of 1.5 bars.

2.5. BSA-FN4C covalent immobilization

The silanized sensor chip was placed on the experimental setup for the *in-situ* immobilization of the BSA-FN4C conjugate through covalent binding of the carboxylic groups introduced on the

surface of the sensor chip and the free amino groups of the BSA carrier protein in the conjugate. First, carboxyl groups were activated by flowing a solution with 0.2 M EDC/0.05 M sulfo-NHS in MES buffer at 20 $\mu\text{L min}^{-1}$ over the sensor surface. Next, a solution of BSA-FN4C conjugate (20 $\mu\text{g mL}^{-1}$ in acetate buffer) was injected at a flow rate of 10 $\mu\text{L min}^{-1}$. The remaining unreacted carboxyl groups were deactivated by passing an ethanolamine solution at 20 $\mu\text{L min}^{-1}$ for 2 min. Milli-Q water was used as the running buffer during the immobilization step and was then switched to PBST (PBST with either 0.05% or 0.5% Tween 20) for the detection of antibody interactions.

2.6. Competitive immunoassay performance

Different stock solutions of FN (from 2.5 mM to 0.978 μM) were prepared in 1,4-dioxane and stored at 4 °C. Working standards were freshly prepared from each stock solution by a 1/500 dilution in the corresponding working buffer (PBS containing 0.05% or 0.5% of Tween 20). The set of FN concentrations were pre-incubated for 10 min with a fixed concentration of antibody (1 $\mu\text{g mL}^{-1}$) at room temperature. The mixture (100 μL) was injected over the biofunctionalized sensor surface at a constant flow rate of 20 $\mu\text{L min}^{-1}$. A NaOH 10 mM solution was employed to completely dissociate the antibody-antigen interaction. Calibration curves were obtained by assaying different FN concentrations (between 5 μM and 1.95 nM, i.e. 1.38 $\mu\text{g mL}^{-1}$ - 0.54 ng mL^{-1}) by triplicate in PBST 0.05% and 0.5%.

2.7. Matrix effect of tap water

The tap water was collected in Bellaterra (Barcelona, Spain) and stored at 4 °C. For the preparation of calibration curves, working standards were prepared in tap water, and diluted (1:1) in PBST 20 mM 0.1% Tween 20 (PBST 2x) to match the same concentration range described above. This mixture was incubated for 10 min with the specific monoclonal antibody and analyzed as previously described.

2.8. Accuracy study

To evaluate the accuracy of the assay, seven spiked samples (S1 – S7) were prepared by a different researcher (blind samples for the analyst) by spiking tap water with known concentrations of FN. Samples were diluted (1:1) in PBST 2x and analyzed as described above. Concentrations were determined by interpolating from the PBST 0.05% standard curve. Accuracy was determined by applying the following equation:

$$\text{Accuracy (\%)} = \frac{[\text{FN}]_{\text{calculated}}}{[\text{FN}]_{\text{real}}} \times 100 \quad (1)$$

2.9. Data analysis

Data were analyzed using Origin 8.0 (OriginLab, Massachusetts, US) and GraphPad Prism 8 (GraphPad Software, US). The phase variation ($\Delta\phi$) considered for all the measurements was the one observed after signal stabilization, once all the sample had completely passed through the sensor chip (*i.e.* $t \sim 600$ s for detection assays and $t \sim 900$ s for the conjugate immobilization). For the curve fitting, the acquired biosensor response was normalized by expressing the phase variation ($\Delta\phi$) of each standard point as the percentage of the maximum response ($\Delta\phi_{\text{max}}$). Calibration curves were plotted as mean and standard deviation (mean \pm SD) of normalized signal after signal stabilization *versus* the logarithm of FN concentration. The data were fitted to a four-parameter logistic regression equation according to the following formula:

$$y = D + \frac{A - D}{1 + \left(\frac{x}{C}\right)^B} \quad (2)$$

where y is the biosensor response, x is the FN concentration, A is the asymptotic maximum corresponding to the signal in the absence of FN, B is the slope of the curve at the inflection point, C is the x value at the inflection point, equivalent to the half-maximal inhibitory concentration

(IC_{50}), and D is the asymptotic minimum corresponding to the background signal. The LOD was calculated as the FN concentration corresponding to 90% of the signal. The working range was set as the interval between 20 and 80% of the normalized signal ($IC_{20} - IC_{80}$).

3. RESULTS AND DISCUSSION

3.1. Optimization of the immunoassay

The selection of the most suitable immunoassay detection format is highly dependent on the analyte properties, being key factors the size, molecular weight, and the number of different epitopes (part of the structure which is recognized by the antibodies) in the structure. In the case of evanescent wave detection sensors, like the BiMW biosensor, response signals depend explicitly on mass changes induced on the sensor surface [34]. Thus the size is the most critical aspect. For large targets, a direct or a sandwich assay can be mostly appropriate. However, for small analytes ($MW < 500$ Da), such as fenitrothion (FN, $MW = 277.23$ Da), its direct binding to the antibody induces changes of the refractive index relatively small for a direct quantification, limiting the sensitivity of the immunoassay. For this reason, a competitive immunoassay is preferred (Figure 2B). In this configuration, a competitor related to the target analyte, which is also recognized by the specific antibodies, is covalently immobilized onto the sensor surface through a carrier protein, known as the assay conjugate. A fixed concentration of the specific monoclonal antibody is incubated with different concentrations of the analyte in solution. The antibody recognizes both the target and the immobilized competitor, which compete for its binding. Therefore, as the FN concentration in solution increases less amount of antibody will bind to the sensor surface, being the signal inversely proportional to the analyte concentration.

In this study, we have produced specific antibodies for the FN pesticide. A hapten containing a suitable spacer arm has been synthesized (FN4C), to facilitate its conjugation to a carrier protein, BSA to elicit adequate immune response, and OVA for monoclonal antibody selection. The BSA-FN4C conjugate, with a hapten to protein molar ratio of 18, was used as the immunosensor competitor, once immobilized in the sensor surface through the remaining free lysine groups of BSA not reacted with the hapten. The BiMW sensor chip was first functionalized with a silane-PEG-COOH and directly placed in the experimental setup for further *in-situ* covalent binding of the conjugate. Carboxylic groups provided by the silane were activated following the well-known EDC/sulfo-NHS chemistry. Next, several parameters directly affecting surface biofunctionalization process and the performance of the immunoassay were evaluated (i.e., immobilization buffer, conjugate and antibody concentrations, and immunoassay buffer).

The pH of the buffer used to prepare the BSA-FN4C solution can play a decisive role, especially in in-flow dynamic reactions as it can favor the local pre-concentration of the ligand on the surface through electrostatic interactions, therefore increasing the yield of the covalent coupling. Modulating the pH to a value slightly below the pI of the protein results in a positive net charge, which can be electrostatically attracted to the negatively charged carboxylic sensor surface. We studied this influence by injecting several solutions of $10 \mu\text{g mL}^{-1}$ BSA-FN4C prepared in different immobilization buffers adjusted at various pHs ranging from 4.0 to 7.4. Acetate buffer 10 mM at pH 5.0 (Figure S1A in the Supporting Information (SI)) was the one resulting in a higher accumulation of the protein conjugate on the surface (i.e., pH very close to the pI of native BSA is at pH 4.5-5), and was then selected for the covalent immobilization. The appropriate concentration of both BSA-FN4C and antibody were then selected following non-competitive assays (without FN). Two concentrations of BSA-FN4C (20 and $50 \mu\text{g mL}^{-1}$) were immobilized

onto the sensor surface. As expected, immobilization signals showed an increasing tendency with a higher concentration (i.e., $\Delta\phi$ of 37 and 87 rad, respectively, see Figure S1B in the SI). For each case, a set of different antibody concentrations ranging between 0.125 and 8 $\mu\text{g mL}^{-1}$ were injected. As shown in Figure S1C, a similar response for the same antibody concentration was obtained regardless of the conjugate concentration immobilized onto the sensor surface. The suitable antibody concentration should guarantee a sufficient signal to allow a broad working range below non-saturation conditions. We did not reach signal saturation in the evaluated antibody range (see Figure S1C), and the signals were very similar and high enough for both BSA-FN4C concentrations. Thus, in order to favor the competition, the lowest concentration of conjugate (20 $\mu\text{g mL}^{-1}$ of BSA-FN4C) was selected in combination with an antibody concentration that induces a signal near 1 rad. This antibody signal is high enough considering the signal-to-noise ratio of the experimental setup to ensure FN detection at low concentrations. Accordingly, a concentration of 1 $\mu\text{g mL}^{-1}$ of the antibody was selected for the performance of the immunoassay. We confirmed the specificity of the binding of the LIBFN4C22 antibody for the biofunctionalized sensor surface by testing a nonspecific mAb at the same concentration (1 $\mu\text{g mL}^{-1}$). As observed in Figure S1D, this control antibody led to a negligible sensor response, demonstrating that the signal comes solely from the specific recognition of the BSA-FN4C conjugate immobilized onto the sensor surface.

The effect of the assay buffer composition on the immunoassay analytical parameters (i.e., LOD, IC_{50} , and working range) was also evaluated. Particularly, PBS solutions with variable Tween 20 percentages (PBST, with 0.0125 – 0.75 % of Tween 20) were tested. Commonly, this surfactant agent is added in the immunoassays to improve the reproducibility among measurements and prevent nonspecific adsorptions. To evaluate its effect during the competition, a set of three different FN concentrations (0, 0.25, and 2 μM) were studied. The selected FN concentrations

allow making a sweep of the complete analyte range, considering that one is high enough to be close to the bottom limit of the curve (maximum inhibition, signal close to zero), another might be close to the dynamic range, and finally, another one that provides the maximum signal (absence of FN). Additionally, an initial pre-incubation of the antibody with each FN concentration during 10 min was fixed. The results are shown in Figure 3, where an evident influence of the Tween percentage in the immunoassay performance can be observed. When comparing all the analyzed ratios, the best results were obtained with PBST 0.05% and 0.5%. The highest maximum signal was observed with 0.5% and 0.75% of Tween but in this latter case, no complete inhibition was observed at the highest FN concentration ($2 \mu\text{M}$). Besides these two cases, the conditions corresponding to 0.05% Tween showed the most promising results (i.e. high maximum signal around 1.5, rad, a total inhibition signal with high FN concentration ($2 \mu\text{M}$), and with a signal reduced more than half for a FN intermediate concentration ($0.25 \mu\text{M}$). Thus, PBST 0.05% and PBST 0.5% were initially selected to perform a complete competitive assay.

Reusability of the biofunctionalized sensor surface, by entirely disrupting LIB-FN4C22 mAb/BSA-FN4C interaction while maintaining the biorecognition layer intact, is one of the main advantages of biosensors over other bioanalytical methods, which can be especially useful for continuous automated monitoring in the environmental field. This can be achieved with changes in the pH or ionic strength of the media. In our case, the regeneration of the sensor surface was accomplished by flowing a 10 mM NaOH solution (Figure S1E). The conditions were strong enough to guarantee the total disruption of the binding but mild enough to ensure high stability of the functionalized sensor surface for more than 120 cycles without significantly reducing the maximum antibody signal (Figure S1F).

With all the above-selected immunoassay parameters, complete calibration curves were carried out with FN concentrations ranging from 1.95 nM to 5 μ M diluted in the two selected buffers (PBST 0.05% and 0.5%). Samples were flowed over the BSA-FN4C coated surface after a pre-incubation of 10 minutes with a fixed concentration of LIB-FN4C22 antibody (1 μ g mL⁻¹). As shown in Figure 4 and Table 1, a clear influence of the Tween percentage in the immunoassay was observed. The PBST with ten times more concentrated Tween 20 (PBST 0.5% Tween) resulted in a significant worsening of the sensitivity of around one order of magnitude (both in the LOD and the IC₅₀). The main analytical parameters for each of the assays are summarized in Table 1. According to these results, PBST 0.05% was finally selected for the evaluation in tap water samples. Under these conditions, a LOD and IC₅₀ of 0.93 nM (0.26 ng mL⁻¹) and 5.88 nM (1.65 ng mL⁻¹) were reached, respectively, and the linear working range was found between 1.84 and 18.74 nM (0.52 and 5.25 ng mL⁻¹). The coefficient of variation (CV) for both intra-assays and inter-assays for the main analytical parameters were well-below 10 and 15%, respectively (see Table 2), which are values commonly acceptable for bioanalytical methods [43]. These results corroborate the excellent reproducibility and low variability of the competitive immunoassay for the detection of FN. The specificity of the antibody, previously evaluated by ELISA measuring the cross-reactivity (CR) with other pesticides having a molecular structure closely related to FN, showed excellent performance as summarized in Table S1. All the compounds exhibited a value lower than 0.1%, except parathion-ethyl that was slightly recognized by the antibody (CR = 2.5%), probably related to its high structural similarity to FN. Nevertheless this cross-reactivity is low and overall the results indicate that LIB-FN4C22 is highly specific against FN.

Table 1. Analytical parameters for the competitive immunoassay for FN in buffer and tap water (1:1).

LOD (IC ₉₀) (ng mL ⁻¹)	IC ₅₀ (ng mL ⁻¹)	Working Range (IC ₈₀ – IC ₂₀)	HillSlope
---	--	---	-----------

			(ng mL ⁻¹)	
PBST 0.05%	0.26	1.65	0.52 – 5.25	-1.195
PBST 0.5%	1.91	24.4	4.89 – 122.3	-0.875
Tap water:PBST 2x (1:1)	0.29	1.71	0.56 – 5.17	-1.251

Table 2. Intra-assay and inter-assay variability of the main analytical parameters for the competitive immunoassay in PBST 0.05%.

	Intra-assay^a		Inter-assay^b	
	Average ± SD	%CV	Average ± SD	%CV
IC₅₀ (ng mL⁻¹)	1.59 ± 0.11	6.82	1.65 ± 0.06	3.74
LOD (ng mL⁻¹)	0.25 ± 0.01	5.84	0.26 ± 0.008	3.26
Δφ_{max} (rad)	1.80 ± 0.02	1.11	1.81 ± 0.03	1.66
HillSlope	-1.15 ± 0.03	2.61	-1.20 ± 0.03	4.17

^a Triplicates within the same biofunctionalized BiMW sensor chip.

^b Triplicates with three different biofunctionalized BiMW sensor chips.

3.2. Analysis in tap water. Accuracy study

Widely used pesticides, including fenitrothion, have the potential to eventually contaminate natural waters and also reach water systems, becoming harmful for humans and other organisms by ingestion or direct contact with them. Then, the feasibility of using the developed immunosensor to analyze water samples was assessed using tap water. To evaluate matrix effects, 1 μg mL⁻¹ of the mAb LIB-FN4C22 was prepared in tap water and injected over the sensor surface. Lower detection signals were observed in comparison with the ones obtained previously in buffer conditions (Figure S2). This result reveals that some water parameters like pH, ionic strength, or the concentration of certain compounds interfere in the assay performance. To correct this effect, samples were diluted 1:1 in PBST 2x (i.e., PBS 20 mM with 0.1% Tween 20). When monitoring the sensor response to the flow of tap water (1:1) in the absence of the antibody, a negligible signal was observed (Figure S2) confirming the lack of any nonspecific adsorption. The same phase variation as in buffer conditions was obtained when the antibody in tap water was diluted 1:1 in

PBST 2x (Figure S2), indicating that buffered tap water does not affect the interaction of the antibody with the hapten immobilized on the sensor surface.

Tap water was spiked with different FN concentrations in the range from 1.95 nM to 5 μ M. The samples were then incubated for 10 minutes with a fixed concentration of the LIB-FN4C22 antibody (1 μ g mL⁻¹), diluted in PBST 2x, before injection onto the BSA-FN4C coated sensor surface. As shown and compared in Figure 5 and Table 1, calibration curves obtained in PBST 0.05% and in tap water samples (1:1) exhibited non-significant differences concerning assay sensitivity. In particular, a LOD of 1.05 nM (0.29 ng mL⁻¹), an IC₅₀ of 6.09 nM (1.71 ng mL⁻¹), and a working range from 2.01 and 18.45 nM (0.56 to 5.17 ng mL⁻¹) were reached for FN detection in tap water samples.

The accuracy of our biosensor for the determination of the FN concentration was then evaluated with tap water samples fortified with FN within and far above the working range of the immunoassay. Seven blind samples (concentration unknown for the researcher performing the analysis) were prepared (S1 – S7). Before the injection over the sensor surface, all samples were diluted 1:1 in PBST 2x (or more if necessary, to fall within the dynamic range, as in the case of samples S1 and S2). The sensor response was monitored in real-time for each analyzed sample (see Figure S3), and the signal was interpolated in the calibration curve obtained for FN (Figure 5). FN concentrations obtained by duplicate with the biosensor were calculated and listed in Table 3. A good correlation was observed between FN concentrations obtained with the biosensor and the real concentration. Accuracy values indicate a slight overestimation (i.e., above 100%) except for the lowest concentration, which is around 80%. Overall, these values are within the accepted accuracy range between 80 – 120%. These results confirm the high accuracy and feasibility of the

developed label-free biosensor to analyze FN in water in less than 20 minutes without the need for any sample pre-treatment.

Overall, we have established a biosensor-based immunoassay for the detection of FN in water with an analytical performance slightly better than some examples reported in the literature using a conventional ELISA (LOD of 0.30 or 0.90 ng mL⁻¹) and electrochemical sensors (LOD of 0.45 and 2.20 ng mL⁻¹), employing different immunoreagents [26,27,31,32]. Furthermore, the high sensitivity and specificity of our methodology for the determination of FN in water samples meet the health-based value imposed for drinking water by WHO (8 µg mL⁻¹) and also the minimum amount set by Australia, as the most restrictive value currently established (7 µg mL⁻¹) [19,44].

Table 3. Accuracy study performed with blind samples with the immunosensor.

Samples	Concentration		Measured ^a ng mL ⁻¹	Accuracy (%)
	nM	Spiked ng mL ⁻¹		
S1	200	55.91	58.32 ± 3.89	104.3
S2	75	20.97	20.48 ± 5.23	97.7
S3	20	5.59	5.67 ± 0.41	101.4
S4	15	4.19	4.80 ± 0.46	114.5
S5	10	2.80	3.09 ± 0.22	110.7
S6	5	1.40	1.10 ± 0.01	78.8
S7	1	0.28	< LOD	-

^a mean ±SD of two measurements

4. CONCLUSIONS

We have developed a biosensor for the straightforward, label-free, and real-time fenitrothion detection in tap water based on a highly sensitive interferometric detection. The strategy consists of a competitive immunoassay format that combines the covalent immobilization of a BSA conjugate carrying FN hapten molecules with specific monoclonal antibodies against the insecticide. The binding of the antibody to the coated sensor surface is inversely proportional to FN concentration in the sample. Several parameters affecting the immunoassay sensitivity have

been optimized, achieving a LOD of 1.05 nM (0.29 ng mL⁻¹) and IC₅₀ of 6.09 nM (1.71 ng mL⁻¹) in tap water with short time-to-result (20 min), which are sufficient for the health-based value calculated for drinking water by WHO (8 µg mL⁻¹). Furthermore, the biosensor accuracy has been evaluated with blind tap water samples showing an excellent correlation with spiked fenitrothion concentrations. Given these promising results, further steps will include the integration of the biosensor in a portable platform, which will promote pushing the technology from laboratory prototypes to compact devices able to perform continuous in-field monitoring of water quality without sample pre-treatment.

ASSOCIATED CONTENT

Supporting Information. Additional figures and tables showing the optimization of several parameters directly affecting the surface biofunctionalization process and the performance of the immunoassay (i.e. immobilization buffer, conjugate and antibody concentrations, and regeneration cycles), analytical parameters for the indirect competitive immunoassay in buffer and tap water, cross-reactivity of the antibody to a set of different pesticides, and finally, sensorgrams showing the detection of FN in tap water blind samples.

AUTHOR INFORMATION

Corresponding Author

* M.- Carmen Estévez – Nanobiosensors and Bioanalytical Applications Group (NanoB2A), Catalan Institute of Nanoscience and Nanotechnology (ICN2), CSIC, CIBER-BBN and BIST, 08193 Barcelona, Spain; e-mail: mcarmen.estevez@icn2.cat

Author Contributions

The manuscript was written through contributions of all authors. All authors have given approval to the final version of the manuscript.

Notes

The authors declare no competing financial interest.

ACKNOWLEDGMENTS

This work received financial support from DIONISOS Project (Retos Colaboración RTC-2017-6222-5). The ICN2 is funded by the CERCA programme / Generalitat de Catalunya. The ICN2 is supported by the Severo Ochoa Centres of Excellence programme, funded by the Spanish Research Agency (AEI, grant no. SEV-2017-0706).

ABBREVIATIONS

ADI, acceptable daily intake; BiMW, bimodal waveguide Interferometer; BSA, bovine serum albumin; CR, cross-reactivity; CV, coefficient of variation; EDC, N-(3-dimethylaminopropyl)-N'-ethylcarbodiimide hydrochloride; ELISA, Enzyme-Linked ImmunoSorbent Assay; FAO, Food and Agriculture Organization; FN, Fenitrothion; IC₅₀, half-maximal inhibitory concentration; LD₅₀, lethal dose; LOD, limit of detection; mAb, monoclonal antibody; OP, Organophosphate; OVA, ovalbumin; PBS, phosphate buffer saline; PBST, PBS with different concentrations of Tween 20; PDMS, polydimethylsiloxane; SD, standard deviation; Si₃N₄, silicon nitride; Silane-PEG-COOH, Triethoxysilane polyethylene glycol carboxylic acid; SPR, Surface Plasmon Resonance; sulfo-NHS, N-hydroxysulfosuccinimide; $\Delta\phi$, phase variation.

REFERENCES

- [1] F. Sánchez-Santed, M.T. Colomina, E. Herrero Hernández, Organophosphate pesticide

exposure and neurodegeneration, *Cortex*. 74 (2016) 417–426.

[2] WHO, Fenitrothion in Drinking-water Background document for development of WHO Guidelines for Drinking-water Quality, 2004.

[3] S.H. Chough, A. Mulchandani, P. Mulchandani, W. Chen, J. Wang, K.R. Rogers, Organophosphorus hydrolase-based amperometric sensor: Modulation of sensitivity and substrate selectivity, *Electroanalysis*. 14 (2002) 273–276.

[4] J.R. Richardson, V. Fitsanakis, R.H.S. Westerink, A.G. Kanthasamy, Neurotoxicity of pesticides, *Acta Neuropathol*. 138 (2019) 343–362.

[5] C. Pope, S. Karanth, J. Liu, Pharmacology and toxicology of cholinesterase inhibitors: Uses and misuses of a common mechanism of action, in: *Environ. Toxicol. Pharmacol.*, Elsevier, 2005: pp. 433–446.

[6] G. Giordano, Z. Afsharinejad, M. Guizzetti, A. Vitalone, T.J. Kavanagh, L.G. Costa, Organophosphorus insecticides chlorpyrifos and diazinon and oxidative stress in neuronal cells in a genetic model of glutathione deficiency, *Toxicol. Appl. Pharmacol*. 219 (2007) 181–189.

[7] Ş. Çakir, R. Sarikaya, Genotoxicity testing of some organophosphate insecticides in the *Drosophila* wing spot test, *Food Chem. Toxicol*. 43 (2005) 443–450.

[8] M.F. Rahman, M. Mahboob, K. Danadevi, B. Saleha Banu, P. Grover, Assessment of genotoxic effects of chloropyriphos and acephate by the comet assay in mice leucocytes, *Mutat. Res. - Genet. Toxicol. Environ. Mutagen*. 516 (2002) 139–147.

[9] S.P. Yeh, T.G. Sung, C.C. Chang, W. Cheng, C.M. Kuo, Effects of an organophosphorus insecticide, trichlorfon, on hematological parameters of the giant freshwater prawn,

Macrobrachium rosenbergii (de Man), *Aquaculture*. 243 (2005) 383–392.

[10] WHO, Specifications and evaluations for public health pesticides: Fenitrothion O,O-dimethyl O-4-nitro-m-tolyl phosphorothioate, 2010.

[11] D. Wang, H. Naito, T. Nakajim, The Toxicity of Fenitrothion and Permethrin, *Insectic. - Pest Eng.* (2012).

[12] FAO/WHO, Fenitrothion (FAO/PL:1969/M/17/1), 2000.

[13] United States Environmental Protection Agency, Reregistration Eligibility Decision for Fenitrothion, 1995.

[14] W. and FAO, Pesticide Residues in Food, 2003.

[15] A.G. Smith, S.D. Gangoli, Organochlorine chemicals in seafood: Occurrence and health concerns, *Food Chem. Toxicol.* 40 (2002) 767–779.

[16] P. Kumar, K.H. Kim, A. Deep, Recent advancements in sensing techniques based on functional materials for organophosphate pesticides, *Biosens. Bioelectron.* 70 (2015) 469–481.

[17] Z. Li, A. Jennings, Worldwide regulations of standard values of pesticides for human health risk control: A review, 2017.

[18] WHO, Guidelines for drinking-water quality, 4th edition, incorporating the 1st addendum, WHO, 2017.

[19] WHO, A global overview of national regulations and standards for drinking-water quality, 2018.

[20] M. Schellin, B. Hauser, P. Popp, Determination of organophosphorus pesticides using

membrane-assisted solvent extraction combined with large volume injection–gas chromatography–mass spectrometric detection, *J. Chromatogr. A.* 1040 (2004) 251–258.

[21] M.E. Sánchez, R. Méndez, X. Gómez, J. Martín-Villacorta, Determination of diazinon and fenitrothion in environmental water and soil samples by HPLC, *J. Liq. Chromatogr. Relat. Technol.* 26 (2003) 483–497.

[22] J. Sherma, Pesticides, *Anal. Chem.* 65 (1993) 40–54. <https://doi.org/10.1021/ac00060a004>.

[23] H. Grigoryan, B. Li, W. Xue, M. Grigoryan, L.M. Schopfer, O. Lockridge, Mass spectral characterization of organophosphate-labeled lysine in peptides, *Anal. Biochem.* 394 (2009) 92–100.

[24] C.M. Thompson, J.M. Prins, K.M. George, Mass spectrometric analyses of organophosphate insecticide oxon protein adducts, *Environ. Health Perspect.* 118 (2010) 11–19.

[25] J. Wang, M.P. Chatrathi, A. Mulchandani, W. Chen, Capillary electrophoresis microchips for separation and detection of organophosphate nerve agents, *Anal. Chem.* 73 (2001) 1804–1808.

[26] E. Watanabe, Y. Kanzaki, H. Tokumoto, R. Hoshino, H. Kubo, H. Nakazawa, Enzyme-linked immunosorbent assay based on a polyclonal antibody for the detection of the insecticide fenitrothion. Evaluation of antiserum and application to the analysis of water samples, *J. Agric. Food Chem.* 50 (2002) 53–58.

[27] X. Hua, J. Yang, L. Wang, Q. Fang, G. Zhang, F. Liu, Development of an Enzyme Linked Immunosorbent Assay and an Immunochromatographic Assay for Detection of Organophosphorus Pesticides in Different Agricultural Products, *PLoS One.* 7 (2012).

[28] G. Liu, Y. Lin, Electrochemical sensor for organophosphate pesticides and nerve agents

using zirconia nanoparticles as selective sorbents, *Anal. Chem.* 77 (2005) 5894–5901.

[29] P.C. Mane, M.D. Shinde, S. Varma, B.P. Chaudhari, A. Fatehmulla, M. Shahabuddin, D.P. Amalnerkar, A.M. Aldhafiri, R.D. Chaudhari, Highly sensitive label-free bio-interfacial colorimetric sensor based on silk fibroin-gold nanocomposite for facile detection of chlorpyrifos pesticide, *Sci. Rep.* 10 (2020) 1–14.

[30] F.Q. Fan, J.F. Dou, L.R. Cheng, A.Z. Ding, L. Jiang, J.J. Yao, Y.C. Du, Y.H. Liu, D. Zhang, Determination of two organophosphorus pesticides using electrochemical sensor in water samples, in: *Adv. Mater. Res.*, Trans Tech Publications Ltd, 2011: pp. 368–371.

[31] A.A. Ensafi, F. Rezaei, B. Rezaei, Electrochemical Determination of Fenitrothion Organophosphorus Pesticide Using Polyzincon Modified-glassy Carbon Electrode, *Electroanalysis.* 29 (2017) 2839–2846.

[32] P. Qi, J. Wang, X. Wang, X. Wang, Z. Wang, H. Xu, S. Di, Q. Wang, X. Wang, Sensitive determination of fenitrothion in water samples based on an electrochemical sensor layered reduced graphene oxide, molybdenum sulfide (MoS₂)-Au and zirconia films, *Electrochim. Acta.* 292 (2018) 667–675.

[33] R. Kant, Surface plasmon resonance based fiber-optic nanosensor for the pesticide fenitrothion utilizing Ta₂O₅ nanostructures sequestered onto a reduced graphene oxide matrix, *Microchim. Acta.* 187 (2020) 1–11.

[34] K.E. Zinoviev, A.B. González-Guerrero, C. Domínguez, L.M. Lechuga, Integrated bimodal waveguide interferometric biosensor for label-free analysis, *J. Light. Technol.* 29 (2011) 1926–1930.

- [35] J. Maldonado, M.C. Estévez, A. Fernández-Gavela, J.J. González-López, A.B. González-Guerrero, L.M. Lechuga, Label-free detection of nosocomial bacteria using a nanophotonic interferometric biosensor, *Analyst*. 145 (2020) 497–506.
- [36] C.S. Huertas, D. Fariña, L.M. Lechuga, Direct and Label-Free Quantification of Micro-RNA-181a at Attomolar Level in Complex Media Using a Nanophotonic Biosensor, *ACS Sensors*. 1 (2016) 748–756.
- [37] J. Maldonado, A.B. González-Guerrero, C. Domínguez, L.M. Lechuga, Label-free bimodal waveguide immunosensor for rapid diagnosis of bacterial infections in cirrhotic patients, *Biosens. Bioelectron*. 85 (2016) 310–316.
- [38] A.B. González-Guerrero, J. Maldonado, S. Dante, D. Grajales, L.M. Lechuga, Direct and label-free detection of the human growth hormone in urine by an ultrasensitive bimodal waveguide biosensor, *J. Biophotonics*. 10 (2017) 61–67.
- [39] B. Chocarro-Ruiz, S. Herranz, A. Fernández Gavela, J. Sanchís, M. Farré, M.P. Marco, L.M. Lechuga, Interferometric nanoimmunosensor for label-free and real-time monitoring of Irgarol 1051 in seawater, *Biosens. Bioelectron*. 117 (2018) 47–52.
- [40] B. Chocarro-Ruiz, J. Pérez-Carvajal, C. Avci, O. Calvo-Lozano, M.I. Alonso, D. MasPOCH, L.M. Lechuga, A CO₂ optical sensor based on self-assembled metal-organic framework nanoparticles, *J. Mater. Chem. A*. 6 (2018) 13171–13177.
- [41] J.J. Manclús, J. Primo, A. Montoya, Development of Enzyme-Linked Immunosorbent Assays for the Insecticide Chlorpyrifos. 1. Monoclonal Antibody Production and Immunoassay Design, *J. Agric. Food Chem*. 44 (1996) 4052–4062.

[42] S. Dante, D. Duval, D. Fariña, A.B. González-Guerrero, L.M. Lechuga, Linear readout of integrated interferometric biosensors using a periodic wavelength modulation, *Laser Photon. Rev.* 9 (2015) 248–255.

[43] FDA, *Bioanalytical Method Validation - Guidance for Industry*, 2018.

Figure legends

Figure 1. Structures of fenitrothion and hapten FN4C.

Figure 2. (A) Photograph of a BiMW sensor chip. Zoom in one of the bimodal waveguides shows a schematic representation of the working principle. **(B)** Representation of the three main steps in the development of a competitive immunoassay for the detection of FN: functionalization of the sensor chip with silane-PEG-COOH; covalent immobilization of hapten-protein conjugate (BSA-FN4C competitor) and competition step with the sample containing a fixed concentration of antibody (LIB-FN4C22) and FN as target analyte.

Figure 3. Results obtained from the indirect competitive immunoassay for different FN concentrations (0, 0.25, and 2 μM) pre-incubated with the antibody in different buffers: PBS and PBST with 0.0125 – 0.75% of Tween 20. $[\text{BSA-FN4C}] = 20 \mu\text{g mL}^{-1}$; $[\text{LIB-FN4C22}] = 1 \mu\text{g mL}^{-1}$. (Each column represents the mean \pm SD of duplicates).

Figure 4. Normalized standard calibration curves of a competitive immunoassay for FN detection in PBST 0.05% (green curve) and PBST 0.5% (purple curve). $[\text{LIBFN4C22}] = 1 \mu\text{g mL}^{-1}$; (Each point represents the mean \pm SD of three replicates).

Figure 5. Calibration curves for FN detection in PBST 0.05% (black) and tap water (1:1, blue). Each point represents the mean \pm SD of three replicates.

Figure 1

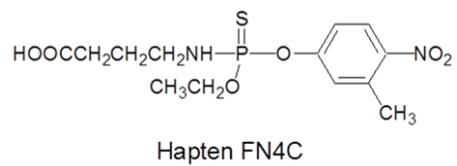
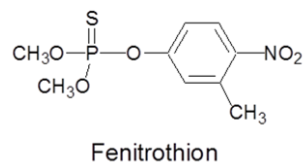


Figure 2

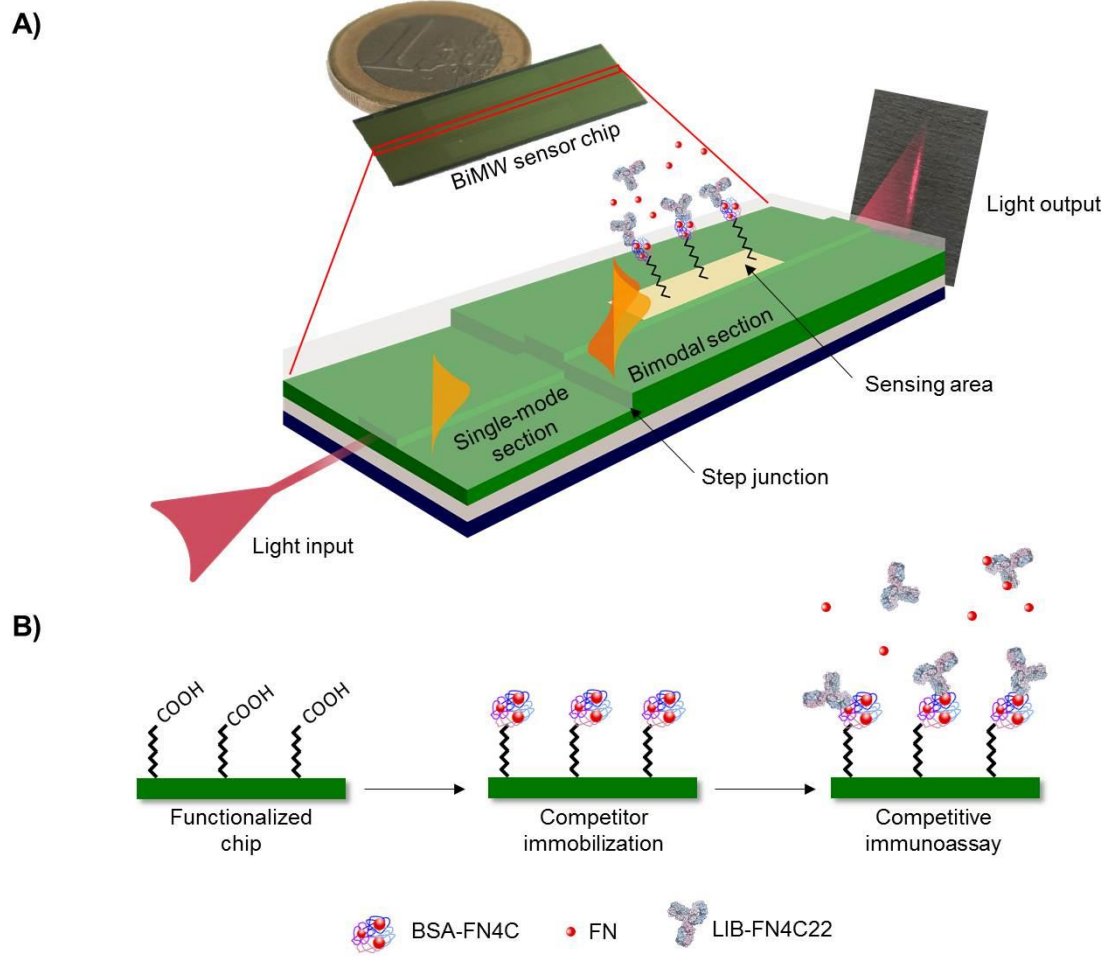


Figure 3

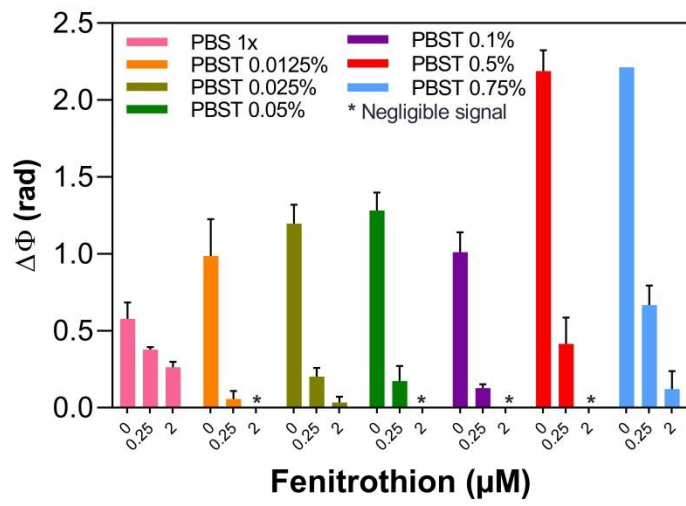


Figure 4

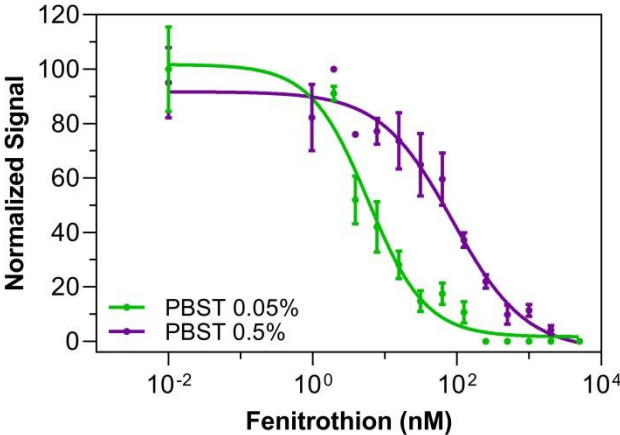


Figure 5

